INTERNATIONAL JOURNAL FOR NUMERICAL METHODS IN FLUIDS, VOL. 24, 1211–1223 (1997)

# A LINEAR THEORY FOR EKMAN'S BOUNDARY LAYER ACCORDING TO A TRIPLE DECK

RACHID KHARAB

*Analyse des Modèles Stochastiques, URA CNRS 1378, Mathématique UFR Sciences, Université de Rouen, F-76821 Mont-Saint-Aignan Cedex, France*

## SUMMARY

The problem of the interaction between Ekman's classical boundary layer and that induced by a thermally non-homogeneous site shows that the latter is strongly linked to the order of magnitude of the horizontal scale of the site.

Our purpose is the analysis of the local interaction equations (Boussinesq equations) starting from a triple-deck model. This analysis yields a system of quasi-linear equations for the viscous lower deck. The linear theory of this system shows that the thermal non-homogeneity has a significant influence on the Ekman boundary layer flow owing to the interactive nature of the triple-deck structure. The numerical solution of the quasi-linear system confirms to a large extent this influence. The numerical results are given in graph form. © 1997 by John Wiley & Sons, Ltd.

*Int. J. Numer. Meth. Fluids*, **24**: 1211–1223, 1997.

No. of Figs: 6. No. of Tables: 0. No. of Refs: 9.

KEY WORDS: Ekman's boundary layer; triple deck; non-homogeneity

## 1. INTRODUCTION

In this article the interaction between an Ekman boundary layer and a local circulation induced by a thermally non-homogeneous site is studied. A generalization of the work of Sykes[1] is thus obtained. This problem is concerned more particularly with meteorology. As a matter of fact, if we wish to regionalize synoptic prediction, i.e. to be able to do local prediction, we have, among other things, to elucidate how a site of horizontal scale $L$ perturbs the Ekman layer. The consistent formulation of this problem of the interaction between the Ekman boundary layer and that induced by a thermally non-homogenous site turns out to be strongly linked to $L$, the order of magnitude of the site. We notice for $L \approx 10^3$ m that an auto-inductive coupling triple-deck scheme developed independently by Stewartson and William[2] and Neiland[3] has to be used. According to Zeytounian,[4] for the local formulation we may then neglect the effect of the Coriolis force and proceed to the Boussinesq approximation.[5]

We begin by describing the triple-deck model obtained by Zeytounian[6] and analysing the equations of the upper layer and the conditions for matching with the viscous lower deck. Then we analyse the linearization of the viscous lower-deck equations. Finally we develop the numerical solution of the non-linear problem and present the results in graph form.

CCC 0271–2091/97/111211–13 $17.50 *Received January 1996*
© 1997 by John Wiley & Sons, Ltd.

## 2. TRIPLE-DECK SCHEME

In the following we consider a two-dimensional stationary problem. This is justified when $L$ is of the order of a few kilometres. We do not take into account the site. Our main purpose is to elucidate to what extent the Ekman layer profile is perturbed by the presence of a thermally non-homogeneous site on the $X$-axis between $X=0$ and $X=L$ as shown in Figure 1.

We can write the following local interaction problem by using the Boussinesq approximation according to Zeytounian:[5]

$$u^* \frac{\partial u^*}{\partial x^*} + w^* \frac{\partial u^*}{\partial z^*} + \frac{1}{\gamma} \frac{\partial \pi^*}{\partial x^*} = \beta^m \Delta^* u^*, \tag{1}$$

$$u^* \frac{\partial w^*}{\partial x^*} + w^* \frac{\partial w^*}{\partial z^*} + \frac{1}{\gamma} \frac{\partial \pi^*}{\partial z^*} - \frac{\delta}{\gamma} \theta^* = \beta^m \Delta^* w^*, \tag{2}$$

$$\frac{\partial u^*}{\partial x^*} + \frac{\partial w^*}{\partial z^*} = 0, \tag{3}$$

$$u^* \frac{\partial \theta^*}{\partial x^*} + w^* \frac{\partial \theta^*}{\partial z^*} + \delta \left( \frac{\gamma - 1}{\gamma} + \frac{\mathrm{d}T_\infty}{\mathrm{d}z} \bigg|_{z=0} \right) w^* = \beta^m \Delta^* \theta^*, \tag{4}$$

with the boundary conditions

$$\begin{aligned} &u^* = w^* = 0, \quad \theta^* = \Lambda F(x), \quad 0 \leqslant x \leqslant 1, \quad \text{at } z^* = 0, \\ &u^* \to U_\infty \left( \frac{z^*}{\beta} \right), \quad (w^*, \pi^*, \theta^*) \to 0, \quad \text{for } x^* \to -\infty. \end{aligned} \tag{5}$$

Here $\beta$ is a small perturbation parameter linked with the Ekman boundary layer, whose expression is

$$\beta^2 = \frac{v_0}{L^2 \Omega_0 \sin \varphi_0} = \frac{2Ro}{Re}, \tag{6}$$

where

$$Re = \frac{LU_0}{v_0} \quad \text{and} \quad Ro = \frac{U_0}{2L\Omega_0 \sin \varphi_0} \tag{7}$$

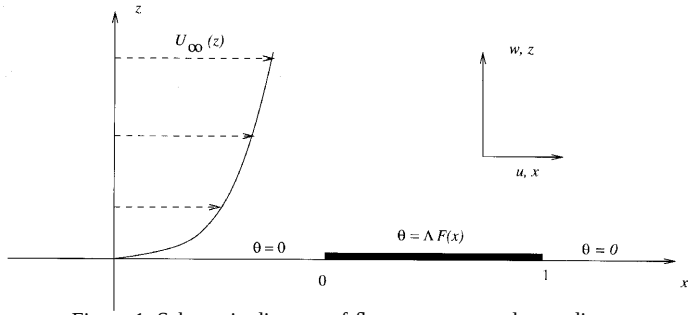


Figure 1. Schematic diagram of flow geometry and co-ordinate system

 © 1997 by John Wiley & Sons, Ltd.

are the local Reynolds and Rossby numbers respectively, based on $L$ and $v_0$, with $v_0$ the kinematic viscosity of the atmosphere. We have

$$z^* = \frac{z}{L}, \qquad x^* = \frac{x}{L}, \qquad (u^*, w^*) = \left(\frac{u}{U_0}, \frac{w}{U_0}\right). \tag{8}$$

$\pi^*$ and $\theta^*$ are the pressure and temperature perturbations respectively and $\delta$ and $\Lambda$ are similitude parameters of order unity. $F(x)$ is given: it is the temperature distribution on the surface of the local site. Finally, $U_\infty$ is the Ekman longitudinal speed profile in the non-dimensional form

$$U_\infty = 1 - \exp\left(-\frac{z^*}{\beta}\right)\cos\left(\frac{z^*}{\beta}\right), \tag{9}$$

with

$$\lim_{z^*/\delta \to \infty} U_\infty\left(\frac{z^*}{\beta}\right) = 1, \qquad \Gamma_\infty(0) = -\left.\frac{\mathrm{d}T}{\mathrm{d}z^*}\right|_{z^*=0},$$

and $\gamma$ is a constant equal to the adiabatic index. When $\beta \to 0$, the local problem (1)–(5) consists of the study of three vertical scales, at least in the self-inductive coupling scheme corresponding to $m = 5$ (Figure 2). The value $m = 5$ is the same as the one used by Smith[7] in his study of the linear flow over a small 'hump' on a plane plaque. This work has been generalized to the three-dimensional case by Smith *et al.*[8] with $m = 5$. Finally, Sykes[1] has used the preceding results to analyse the stratification effects on a Boussinesq fluid in the boundary layer flow over a small mountain whose spread is of the order of 1·5 km and maximum height 60 m.

*Middle deck*

In this deck we have the asymptotic representation

$$\begin{aligned} u^* &= U_\infty(\bar{z}) + \beta\bar{u} + O(\beta^2), & w^* &= \beta^2\bar{w} + O(\beta^3), \\ \pi^* &= \beta^2\bar{\pi} + O(\beta^3), & \theta^* &= \beta\bar{\theta} + O(\beta^2), \end{aligned} \tag{10}$$

where $\bar{z} = \tilde{z}/\beta$. The components $\bar{u}$ and $\bar{w}$ satisfy the classical system

$$U_\infty(\bar{z})\frac{\partial\bar{u}}{\partial x} + \frac{\mathrm{d}U_\infty}{\mathrm{d}\bar{z}}\bar{w} = 0, \tag{11}$$

$$\frac{\partial\bar{u}}{\partial x} + \frac{\partial\bar{w}}{\partial\bar{z}} = 0, \tag{12}$$

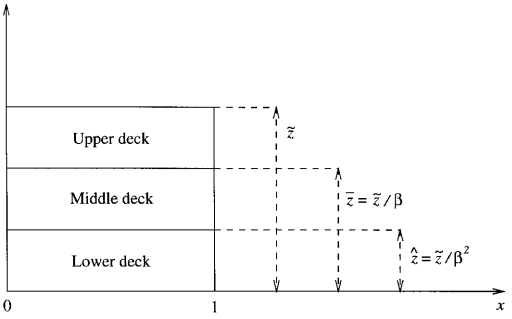


Figure 2. Definition sketch of asymptotic regions and stretched vertical co-ordinates for triple-deck analysis

© 1997 by John Wiley & Sons, Ltd. 

whose solution is

$$\bar{u} = A(x)\frac{\mathrm{d}U_\infty}{\mathrm{d}\bar{z}}, \qquad \bar{w} = -\frac{\mathrm{d}A}{\mathrm{d}x}U_\infty(\bar{z}), \tag{13}$$

where the function $\beta A(x)$ should be interpreted as a thickness displacement which, as a matter of fact, generates the pressure perturbation.

*Lower deck*

$$\begin{aligned} u^* &= \beta\hat{u} + O(\beta^2), & w^* &= \beta^3\hat{w} + O(\beta^4),\\ \pi^* &= \beta^2\hat{\pi} + O(\beta^3), & \theta^* &= \hat{\theta} + O(\beta). \end{aligned} \tag{14}$$

Substituting these expressions in (1)–(5) and retaining only comparable terms, the following system is obtained:[6]

$$\hat{u}\frac{\partial\hat{u}}{\partial x} + \hat{w}\frac{\partial\hat{u}}{\partial\hat{z}} + \frac{\delta}{\gamma}\int_\infty^{\hat{z}} \frac{\partial\hat{\theta}}{\partial x}\mathrm{d}z + \frac{1}{\gamma}\frac{\partial P}{\partial x} = \frac{\partial^2\hat{u}}{\partial\hat{z}^2}, \tag{15}$$

$$\frac{\partial\hat{u}}{\partial x} + \frac{\partial\hat{w}}{\partial\hat{z}} = 0, \tag{16}$$

$$\hat{\pi} = \delta\int_\infty^{\hat{z}} \hat{\theta}\mathrm{d}z + P(x), \tag{17}$$

$$\hat{u}\frac{\partial\hat{\theta}}{\partial x} + \hat{w}\frac{\partial\hat{\theta}}{\partial\hat{z}} = \frac{1}{Pr}\frac{\partial^2\hat{\theta}}{\partial\hat{z}^2}, \tag{18}$$

with the boundary conditions

$$\begin{gathered} \hat{u} = \hat{w} = 0, \quad \hat{\theta} = \Lambda F(x), \quad 0 \leqslant x \leqslant 1, \quad \text{at } z^* = 0,\\ \hat{u} \to \hat{z}, \quad (\hat{w}, P, \hat{\theta}) \to 0, \quad \text{for } x \to -\infty,\\ \hat{u} \to \hat{z} + A(x), \quad \hat{w} \to -\hat{z}\frac{\mathrm{d}A}{\mathrm{d}x}, \quad \hat{\theta} \to 0, \quad \text{for } \hat{z} \to \infty,\\ A(-\infty) = \frac{\mathrm{d}A}{\mathrm{d}x}(-\infty) = 0. \end{gathered} \tag{19}$$

The strong singular self-induction arises because the problem (15)–(18) to be solved in the lower viscous layer does not accept $P(x)$ as data known prior to the resolution (as is the case in classical boundary layer problems). It has to be calculated simultaneously with the velocity components $u$ and $w$ and the temperature perturbation $\theta$

It should be emphasized, however, that this pressure perturbation $P(x)$ is not completely arbitrary. It is connected to the function $A(x)$ in a manner determined by the analysis of the upper deck flow.

*Upper deck*

In this deck we formulate the asymptotic representation

$$\begin{aligned} u^* &= 1 + \beta\tilde{u} + O(\beta^2), & w^* &= \beta^2\tilde{w} + O(\beta^3),\\ \pi^* &= \beta^2\tilde{\pi} + O(\beta^3), & \theta^* &= \beta^2\tilde{\theta} + O(\beta^3). \end{aligned} \tag{20}$$

 © 1997 by John Wiley & Sons, Ltd.

We then obtain the following linear system for $\tilde{u}, \tilde{w}, \tilde{\pi}$ and $\tilde{\theta}$:

$$\frac{\partial \tilde{u}}{\partial x} + \frac{1}{\gamma}\frac{\partial \tilde{\pi}}{\partial x} = 0, \tag{21}$$

$$\frac{\partial \tilde{w}}{\partial x} + \frac{1}{\gamma}\frac{\partial \tilde{\pi}}{\partial \tilde{z}} = \frac{\delta}{\gamma}\tilde{\theta}, \tag{22}$$

$$\frac{\partial \tilde{u}}{\partial x} + \frac{\partial \tilde{\pi}}{\partial \tilde{z}} = 0, \tag{23}$$

$$\frac{\partial \tilde{\theta}}{\partial x} + \delta\left(\frac{\gamma - 1}{\gamma} + \frac{\mathrm{d}T_\infty}{\mathrm{d}\tilde{z}}\bigg|_{z=0}\right)\tilde{w} = 0. \tag{24}$$

Eliminating all these functions except $\tilde{\pi}(x, \tilde{z})$ in (21)–(24) yields the following Helmholtz equation for $\tilde{\pi}$:

$$\left(\frac{\partial^2}{\partial x^2} + \frac{\partial^2}{\partial \tilde{z}^2} + \mu_0^2\right)\frac{\partial \tilde{\pi}}{\partial x} = 0, \tag{25}$$

where

$$\mu_0^2 = \frac{\delta}{\gamma}\left(\frac{\gamma - 1}{\gamma} + \frac{\mathrm{d}T_\infty}{\mathrm{d}\tilde{z}}\bigg|_{z=0}\right) > 0. \tag{26}$$

At $\tilde{z} = 0$ the solution (25) must verify

$$\tilde{\pi}(x, 0) = P(x), \qquad \tilde{w}(x, 0) = -\frac{\mathrm{d}A}{\mathrm{d}x}, \tag{27}$$

i.e.

$$\frac{\partial}{\partial x}\left(\frac{\partial \tilde{\pi}}{\partial x}\bigg|_{\tilde{z}=0}\right) = \gamma\left(\mu_0^2\frac{\mathrm{d}A}{\mathrm{d}x} + \frac{\mathrm{d}^3A}{\mathrm{d}x^3}\right). \tag{28}$$

If $\pi^*(k, z)$ denotes the Fourier transform of $\pi(x, z)$, i.e.

$$\pi^*(k, z) = \int_{-\infty}^{\infty} \pi(x, z)\mathrm{e}^{-\mathrm{i}kx}\mathrm{d}x,$$

we obtain the solution of (25)–(27) as

$$\pi^*(k, z) = P^*(k)\mathrm{e}^{\mathrm{i}mz}, \tag{29}$$

where

$$m = \begin{cases} \mathrm{i}(k^2 - \mu_0^2)^{1/2}, & |k| < \mu_0, \\ (\mu_0^2 - k^2)^{1/2}, & |k| < \mu_0. \end{cases} \tag{30}$$

From (27) and (28) we obtain the following relation between $A^*(k)$ and $P^*(k)$ in the Fourier plane:

$$A^*(k) = \frac{\mathrm{i}m}{\gamma}\frac{P^*(k)}{\mu_0^2 - k^2}. \tag{31}$$

© 1997 by John Wiley & Sons, Ltd. 

## 3. LINEAR THEORY

First note that equations (15)–(19) and (31) are almost identical with those obtained by Sykes[1] in order to study the effects of stratification due to the boundary layer flow over a small mountain. The only differences are that in equations (15)–(19) there is no effect of the normal velocity component $v$ and that the supplementary term governing the temperature $\int_{\infty}^{\hat{z}} (\partial\hat{\theta}/\partial x)\,\mathrm{d}\hat{z}$ in equation (15) describes the quantity of motion.

More precisely, problem (15)–(19) with constraint (31) is equivalent to Sykes' problem with $\hat{\theta} = 0$, which is equivalent to assuming $\Lambda = 0$. In this case we have to introduce at least a contour and write the adherence conditions on $z = h(x)$, taking into account the parameter in the form $\eta = h_0/L = \beta^2$, where $h_0 = \max|h|$. If no hypothesis is made on the similitude parameter $\Lambda$, problem (15)–(19) with (31) is still non-linear and can only be solved numerically.

The linearization of system (15)–(19) with (31) consists of assuming $\Lambda \ll 1$ and finding the solution in the form

$$\hat{u} = \hat{z} + \Lambda u + O(\Lambda^2), \qquad (\hat{w}, \hat{\theta}, A, P, ) = \Lambda(w, \theta, A, P). \tag{32}$$

Substituting this in (15)–(19) and (31) and retaining only terms of his first order in $\Lambda$, we obtain the linear system (after deleting the 'hats')

$$u\frac{\partial u}{\partial x} + w + \frac{\delta}{\gamma}\int_{\infty}^{z} \frac{\partial\theta}{\partial x}\mathrm{d}z + \frac{1}{\gamma}\frac{\partial P}{\partial x} = \frac{\partial^2 u}{\partial z^2}, \tag{33}$$

$$\frac{\partial u}{\partial x} + \frac{\partial w}{\partial z} = 0, \tag{34}$$

$$z\frac{\partial\theta}{\partial x} = \frac{1}{Pr}\frac{\partial^2\theta}{\partial z^2}, \tag{35}$$

with the boundary conditions

$$\begin{aligned} u = w = 0, \quad \theta = F(x), \quad 0 \leqslant x \leqslant 1, \quad \text{at } z = 0, \\ (w, P, \theta, P) \to 0, \quad \text{for } x \to -\infty, \\ u \to A(x), \quad w \to -z\frac{\mathrm{d}A}{\mathrm{d}x}, \quad \theta \to 0, \quad \text{for } z \to \infty, \\ A(-\infty) = \frac{\mathrm{d}A}{\mathrm{d}x}(-\infty) = 0. \end{aligned} \tag{36}$$

To solve problem (33)–(36), we shall assume that $\delta = 1$ and $Pr = 1$.

Using Fourier transform with respect to $x$, we obtain the following equation for the temperature:

$$\frac{\partial^2\theta^*}{\partial z^2}(k, z) - \mathrm{i}kz\theta^*(k, z) = 0, \tag{37}$$

which has the solution

$$\theta(x, z) = \frac{1}{2\pi Ai^*(0)}\int_{-\infty}^{\infty} Ai((\mathrm{i}k)^{1/3}z)F^*(k)\mathrm{e}^{\mathrm{i}kx}\mathrm{d}k, \tag{38}$$

where $Ai$ is Airy's function of the first kind and $\mathrm{i}^2 = -1$.

From (33) we obtain for $u^*(k, z)$

$$\frac{\partial^3 u^*}{\partial t^3} - t\frac{\partial u^*}{\partial t} = \frac{1}{\gamma}\frac{F^*(k)}{Ai(0)}A_1(t), \qquad t = (\mathrm{i}k)^{1/3}z, \tag{39}$$

 © 1997 by John Wiley & Sons, Ltd.

whose general solution is

$$u^*(k,z) = C(k)\int_0^z Ai((\mathrm{i}k)^{1/3}z)\mathrm{d}z + \frac{1}{\gamma}(\theta^*(k,z) - F^*(k)), \tag{40}$$

where

$$C(k) = 3\frac{\mathrm{i}m}{\gamma}\frac{P^*(k)}{\mu_0^2 - k^2} + \frac{3}{\gamma}F^*(k). \tag{41}$$

Using the other boundary conditions, we obtain the expressions for the pressure $P^*(k)$ and the displacement thickness $A^*(k)$:

$$P^*(k) = \frac{DF^*(k)}{\alpha^{-4/3}(\mathrm{i}k)^{1/3} + \mathrm{i}m/(\mu_0^2 - k^2)}, \tag{42}$$

$$A^*(k) = \frac{\mathrm{i}m}{\gamma}\frac{DF^*(k)}{\alpha^{-4/3}(\mathrm{i}k)^{1/3}(\mu_0^2 - k^2) + \mathrm{i}m}, \tag{43}$$

with

$$\alpha = (-3Ai(0))^{3/4} = 0{\cdot}8272, \qquad D = (3Ai(0)\alpha^{4/3})^{-1} = 0{\cdot}382,$$

where $m$ is determined by relation (30).

*Results*

The asymptotic behaviour of $A(x)$ for large values of $x$, i.e. for $x \gg 1$, is given by

$$A(x) \approx \frac{D}{\gamma}F(x). \tag{44}$$

Figures 3 and 4 represent the graphs of $P(x)$ and $A(x)$ computed numerically using FFT for a temperature profile defined by

$$F(x) = \begin{cases} (1-x^2)^2, & |x| < 1, \\ 0, & |x| \geqslant 1, \end{cases} \tag{45}$$

where we chose $\mu_0 = 0{\cdot}0$ and $2{\cdot}0$

## 4. NUMERICAL MODEL

When $\Lambda = O(1)$, system (15)–(19) with constrain (31) is non-linear and can only be solved numerically. We apply the finite difference method with a Crank–Nicolson scheme, using a non-linear relaxation[7,9] for each space step and an initialization of the function $A(x)$ starting from the linear theory. This method is the same as used by Sykes[1] for the boundary layer flow over hills. The computation of $u_{i+1,j}$ and $\theta_{i+1,j}$ at the point $(x_{i+1}, z_j)$ is done in three stages, using the values of $u_{i-1,j}$, $u_{i,j}$, $\theta_{i-1,j}$ and $\theta_{i,j}$ which are known for $j = 1, \ldots, N$.

The computations are almost identical with those of Sykes[1] and we indicate only the approximation of the terms where $\theta$ intervenes.

© 1997 by John Wiley & Sons, Ltd. 

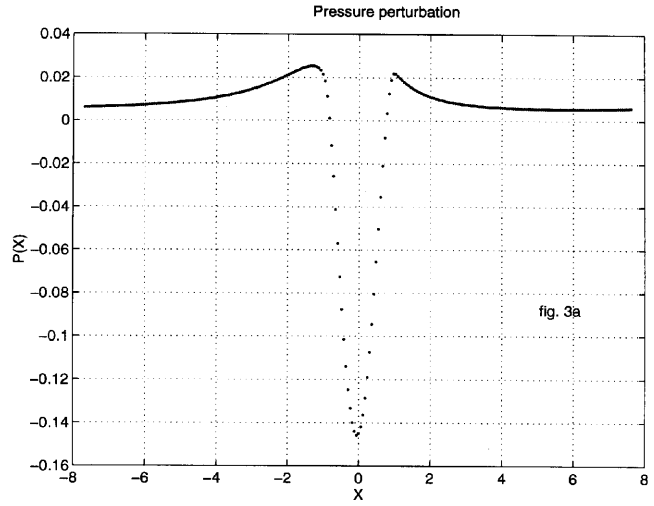


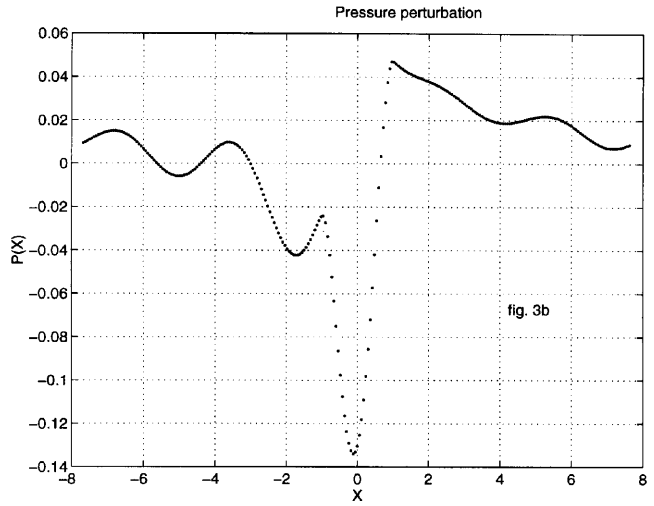


Figure 3. Pressure perturbation from linear case with $\mu_0 = (3a)\ 0{\cdot}0$ and (3b) $2{\cdot}0$

*Stage 1*

Starting from equation (15), we elaborate an explicit method to compute $\tilde{u}_{i+1/2,j}$, a first estimate of the speed. The term $H = (1/\gamma)\int_{\infty}^{z} (\partial\theta/\partial x)\,\mathrm{d}z$ is approximated by trapezoidal rule, using a backward difference formula for $\partial\theta/\partial x$, i.e.

$$H_{i,j} = \frac{\delta z}{\delta x}\frac{1}{\gamma}\left(\sum_{r=2}^{j=1}(\theta_{i,r} - \theta_{i-1,r}) + \tfrac{1}{2}(\theta_{i,j} - \theta_{i-1,j})\right). \tag{46}$$

 © 1997 by John Wiley & Sons, Ltd.

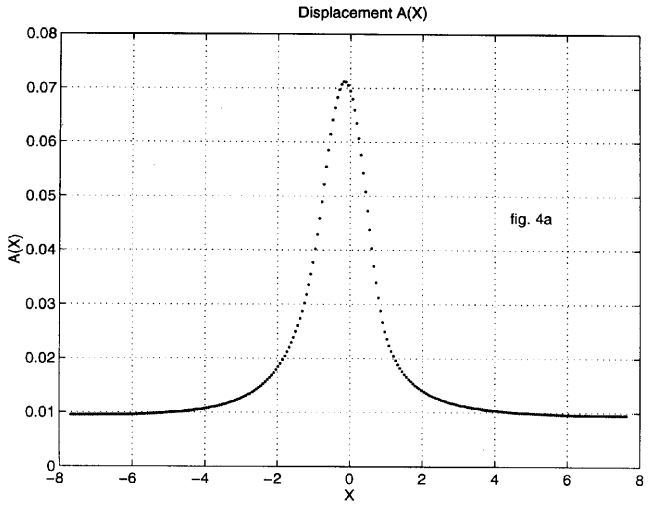


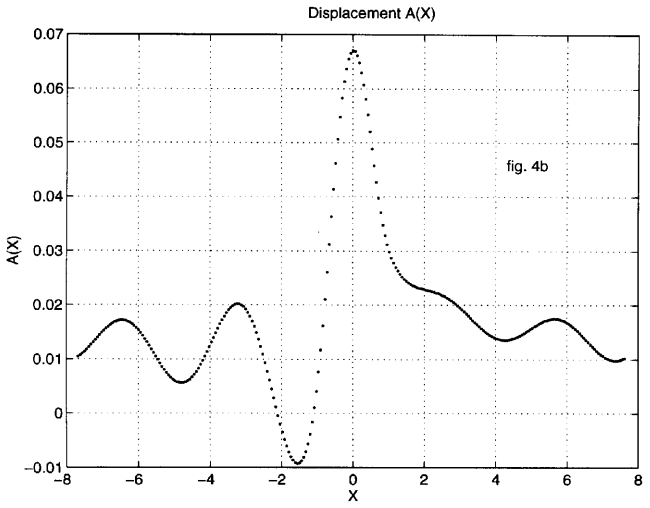


Figure 4. Displacement from linear case with $\mu_0 = (4a)\ 0{\cdot}0$ and $(4b)\ 2{\cdot}0$

The value of $\tilde{u}_{i+1/2,j}$ which we obtain is used to compute a first estimate $\tilde{\theta}_{i+1/2,j}$ of the temperature starting from (18):

$$\left(\frac{u_{i,j}}{\delta x}+\frac{1}{Pr}\frac{1}{\delta z^2}\right)\tilde{\theta}_{i+1/2,j}=\frac{u_{i,j}}{\delta x}\theta_{i-1/2,j}-\left(w_{i,j-1/2}+\frac{\delta z}{\delta x}(u_{i-1/2,j}-\tilde{u}_{i+1/2,j})\right)\frac{\theta_{i,j+1}-\theta_{i,j-1}}{2\delta z}$$
$$+\frac{1}{\delta z^2}(\theta_{i,j+1}-\theta_{i-1/2,j}+\theta_{i,j-1}), \tag{47}$$

© 1997 by John Wiley & Sons, Ltd. 

where the vertical speed is computed from the continuity equation

$$w_{i,j-1/2} = \frac{\delta z}{\delta x} \sum_{r=2}^{j-1} (u_{i-1/2,j} - \tilde{u}_{i+1/2,j}). \tag{48}$$

*Stage 2*

Here the values of $\tilde{u}_{i+1/2,j}$ and $\tilde{\theta}_{i+1/2,j}$ are used to obtain first estimates of the speed, $\tilde{u}_{i+1,j}$, and the temperature, $\tilde{\theta}_{i+1,j}$, at the point $(x_{i+1}, z_j)$. This step and the previous one are identical. It is sufficient to replace $i$ by $i + 1/2$.

*Stage 3*

In this last stage an explicit scheme and the values of $\tilde{u}_{i+1,j}$ and $\tilde{\theta}_{i+1,j}$ are used for calculating $u_{i+1,j}$ and $\theta_{i+1,j}$. Having computed the term $u_{i+1,j}$, we determine $\theta_{i+1,j}$. The temperature equation can then be put in the matrix form

$$C\theta = D, \tag{49}$$

$$\theta = (\theta_{i+1,2}, \ldots, \theta_{i-1,N-1}), \tag{50}$$

where $C$ is a tridiagonal matrix.

We end by determining the pressure field and the new displacement field $A$ starting from (31). The adjustment of the displacement field $A$ is given by

$$A_i^{\text{new}} = (1 - \alpha)A_i^{\text{old}} + \alpha A_i^{\text{calc}}, \tag{51}$$

where $0 \leqslant \alpha < 1$.[9] The iteration is complete when

$$\max_i |A_i^{\text{calc}} - A_i^{\text{old}}| < 5 \times 10^3 \max_i |A_i^{\text{old}}|. \tag{52}$$

## 5. ANALYSIS OF NUMERICAL RESULTS

In this section we present the numerical results for a temperature profile given by

$$F(x) = \begin{cases} \Lambda(1 - x^2)^2, & |x| < 1, \\ 0 & |x| \geqslant 1. \end{cases} \tag{53}$$

Figure 5 illustrates the pressure perturbation and displacement perturbation for various values of the parameters $\Lambda$ and $\mu_0$. We notice that the graphs of $P(x)$ above the thermally non-homogeneous site are concentrated in the domain $|x| \leqslant 1$ and that the minima are negative and located on the same straight line. The pressure of the thermally non-homogeneous site in the flow produces a separation which varies in a regular way. This phenomenon is the same as that observed by Sykes.[1] As a matter of fact, these results are the same as those by linear analysis.

Figure 6c presents the perturbation of the temperature $\theta(x_0, z)$ for $x_0$ fixed in $[-1, 1]$, $\mu_0 = 3{\cdot}0$ and $\Lambda = 2{\cdot}0$. The various plots obtained constitute a good illustration that the temperature profile is perturbed within the thermally non-homogeneous site. Figure 6c shows the temperature perturbation with respect to $z$ for values of $x_0$ between $-0{\cdot}30$ and $0{\cdot}30$ with a step of $0{\cdot}12$. Figures 6a and 6b

 © 1997 by John Wiley & Sons, Ltd.

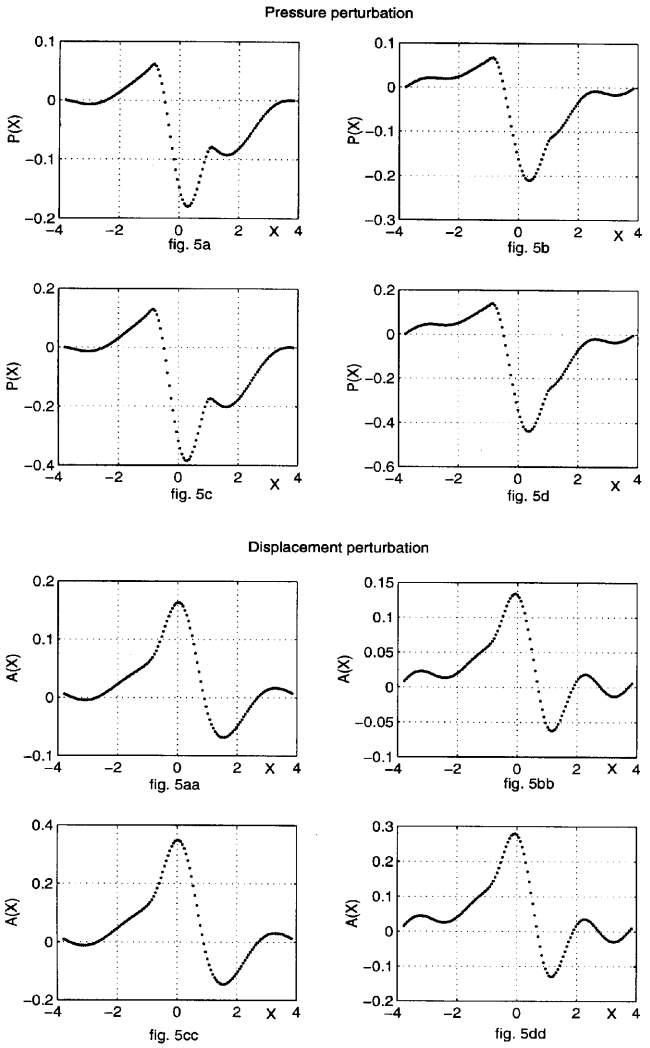


Figure 5. Pressure perturbation and displacement perturbation from numerical solution with (5a, 5aa) $\Lambda = 1{\cdot}0$, $\mu_0 = 2{\cdot}0$, (5b, 5bb) $\Lambda = 1$, $\mu_0 = 3{\cdot}0$, (5c, 5cc) $\Lambda = 2{\cdot}0$, $\mu_0 = 2{\cdot}0$ (5d, 5dd) and $\Lambda = 2{\cdot}0$, $\mu_0 = 3{\cdot}0$ for $\delta x = 0{\cdot}06$, $\delta y = 0{\cdot}08$, $M = 256$ and $N = 60$

present the temperature perturbation as a function of $x$ and $z$ for different values of the parameters $\Lambda$ and $\mu_0$.

All these figures illustrate very clearly the effects of a thermally non-homogeneous site on the basic flow.

## 6. CONCLUSIONS

The linear analysis allows the initialization of the iterative process utilized for the numerical solution of system (15)–(18) when the parameter $\Lambda = O(1)$. The results show that the presence of a thermally non-homogeneous site has a significant influence on the flow of Ekman's classical boundary layer owing to the interactive nature of the triple-layer structure. It should also be noted that the results tally with those obtained by Sykes[1] when $\theta = 0$ and $m = 5$.

© 1997 by John Wiley & Sons, Ltd. 

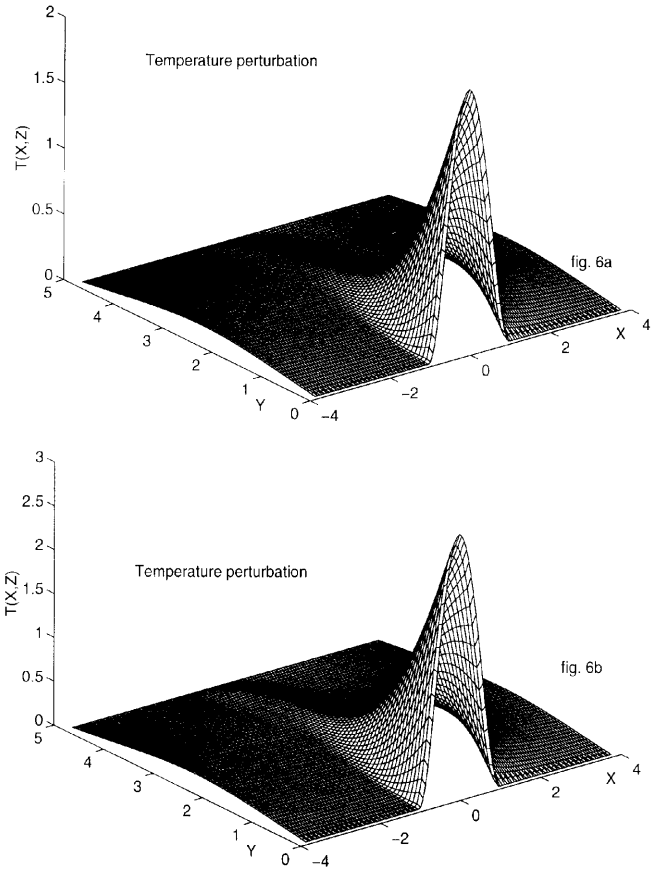


Figure 6a,b. Three-dimensional temperature perturbation from numerical solution with (6a) $\Lambda = 2{\cdot}0$, $\mu_0 = 3{\cdot}0$ and (6b) $\Lambda = 3{\cdot}0$, $\mu_0 = 2{\cdot}0$ for $\delta x = 0{\cdot}06$, $\delta y = 0{\cdot}08$, $M = 256$ and $N = 60$

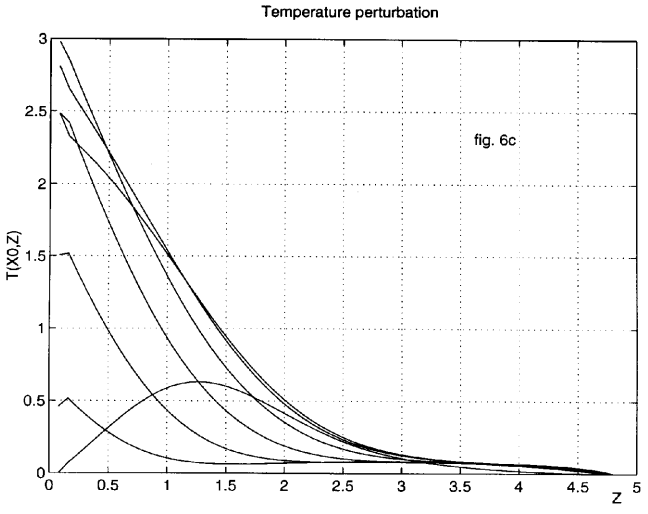


Figure 6c. Curves of temperature perturbation $\theta(x_0, z)$ for fixed $x_0 = -0{\cdot}30, \ldots, 0{\cdot}30$ with respect to $z$, with $\Lambda = 3{\cdot}0$ and $\mu_0 = 2{\cdot}0$

 © 1997 by John Wiley & Sons, Ltd.

ACKNOWLEDGEMENT

I should like to thank Dr. José de Sam Lazaro (University of Rouen) for his help.

REFERENCES

1. R. I. Sykes, *Proc. R. Soc. Lond. A*, **361**, 225–243 (1978).
2. K. Stewartson and P. G. William, *Proc. R. Soc. Lond. A*, **312**, 181–206 (1969).
3. V. Ya. Neiland, *Izv. Akad. Nauk. SSSR Mekh. Zhid. Gaza*, **4**, 4 (1969).
4. R. Kh. Zeytounian, *Int. J. Eng. Sci.*, **23**, 1239–1288 (1985).
5. R. Kh. Zeytounian, *Arch. Mekh. Stosowanej*., **26**, 499 (1974).
6. R. Kh. Zeytounian *Les Modèles Asymptotiques de la Mécanique des Fluides II*, LNP Vol. 276, Springer, Berlin, 1987.
7. F. T. Smith, *Fluid Mech.*, **57**, 803 (1973).
8. F. T. Smith, R. I. Sykes and P. W. M. Brighton, *J. Fluid Mech.*, **83**, 163 (1977).
9. C. E. Jobe and O. R. Burggraf, *Proc. R. Soc. Lond. A*, **340**, 91 (1974).

© 1997 by John Wiley & Sons, Ltd. 